JOC Article
pubs.acs.org/joc

Chemiluminogenic Features of 10-Methyl-9-(phenoxycarbonyl)acridinium Trifluoromethanesulfonates Alkyl Substituted at the Benzene Ring in Aqueous Media

Karol Krzymiński,*[,†] Agnieszka Ożóg,[†] Piotr Malecha,[†] Alexander D. Roshal,[‡] Agnieszka Wróblewska,[†] Beata Zadykowicz,[†] and Jerzy Błażejowski[†]

[†]*Faculty of Chemistry, University of Gdańsk, J. Sobieskiego 18, 80-952 Gdańsk, Poland, and* [‡]*Institute of Chemistry, Kharkiv V.N. Karazin National University, Svoboda 4, 61077 Kharkiv, Ukraine*

karolk@chem.univ.gda.pl

Received October 29, 2010

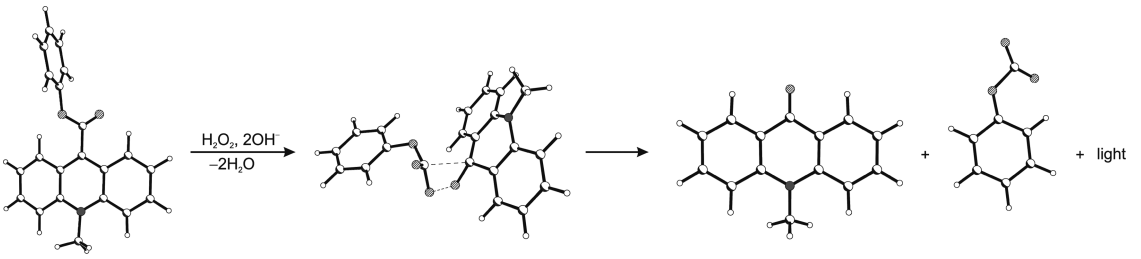

10-Methyl-9-(phenoxycarbonyl)acridinium trifluoromethanesulfonates bearing alkyl substituents at the benzene ring were synthesized, purified, and identified. In the reaction with OOH^- in basic aqueous media, the cations of the compounds investigated were converted to electronically excited 10-methyl-9-acridinone, whose relaxation was accompanied by chemiluminescence (CL). The kinetic constants of CL decay, relative efficiencies of light emission, chemiluminescence quantum yields, and resistance toward alkaline hydrolysis were determined experimentally under various conditions. The mechanism of CL generation is considered on the basis of thermodynamic and kinetic parameters of the reaction steps predicted at the DFT level of theory. The chemiluminescence efficiency is the result of competition of the electrophilic center at C(9) between nucleophilic substitution by OOH^- or OH^- and the ability of the intermediates thus formed to decompose to electronically excited 10-methyl-9-acridinone. Identification of stable and intermediate reaction products corroborated the suggested reaction scheme. The results obtained, particularly the dependency of the "usefulness" parameter, which takes into account the CL quantum yield and the susceptibility to hydrolysis, on the cavity volume of the entity removed during oxidation, form a convenient framework within which to rationally design chemiluminescent 10-methyl-9-(phenoxycarbonyl)acridinium cations.

Introduction

Acridinium derivatives are readily oxidized with hydrogen peroxide,[1] persulfates,[1b] and other oxidants[2] in alkaline media leading to chemiluminescence (CL). The light-emitting species are electronically excited 9-acridinones formed as a result of the decomposition of the addition products of OOH^- to acridinium cations.[2a,3,4] This feature of acridinium salts has prompted their use as chemiluminescent indicators or chemiluminogenic fragments of labels in medical,[5] biochemical,[5e,6] chemical,[7] and environmental[8] analyses. They have been employed in quantitative immunoassays of antigens, antibodies, or hormones with detection limits at the subattomole levels (detection limits as low as 10^{-17} M have been reported).[5c,e] They can also be used to determine concentrations of highly reactive entities occurring in living matter, such as OOH^-.[7,8] They have been successfully applied in flow-injection techniques,[7] cellular studies, and nucleic acid diagnostics,[9] as well as in electrochemiluminogenic assays of

(1) (a) McCapra, F. In *Chemistry of Heterocyclic Compounds*; Acheson, R. M., Ed.; Wiley: New York, 1973; Vol. 9 (Chemiluminescent Reactions of Acridines), pp 615−630. (b) Gundermann, K. D.; McCapra, F. In *Reactivity and Structure Concepts in Organic Chemistry*; Springer-Verlag: Berlin, Heidelberg, 1987; Vol. 23 (Chemiluminescence in Organic Chemistry); pp 109−118. (c) Zomer, G.; Stavenuiter, J. F. C.; Van den Berg, R. H.; Jansen, E. H. J. M. *Pract. Spectrosc.* **1991**, *12*, 505–521.

(2) (a) Yang, M.; Liu, C.; Hu, X.; He, P.; Fang, Y. *Anal. Chim. Acta* **2002**, *461*, 141–146. (b) Wroblewska, A.; Huta, O. M.; Patsay, I. O.; Petryshyn, R. S.; Blazejowski, J. *Anal. Chim. Acta* **2004**, *507*, 229–236. (c) Aizawa, M.; Ikariyama, Y.; Kobatake, E.; Ogasawara, M.; Tanaka, M. Luminescence by reacting an acridinium ester with superoxide. United States Reissued Patent, US RE39,047 E, Mar 28, 2006. (d) Lai, Y.; Qi, Y.; Wang, J.; Chen, G. *Analyst* **2009**, *134*, 131–137. (e) He, Y.; Zhang, H.; Chai, Y.; Cui, H. *Anal. Bioanal. Chem.* **2010**, DOI: 10.1007/s00216-010-4157-y.

(3) McCapra, F. *Pure Appl. Chem.* **1970**, *24*, 611–629.

(4) Rak, J.; Skurski, P.; Blazejowski, J. *J. Org. Chem.* **1999**, *64*, 3002–3008.

Published on Web 01/19/2011 DOI: 10.1021/jo1020882

substances.[2a,c] Acridinium salts exhibit a higher chemiluminescence quantum yield in aqueous media relative to luminol derivatives and, unlike the latter systems, do not require a catalyst to cause the emission of light.[1,5] For these reasons, numerous commercially available chemiluminescent labels contain a 9-(phenoxycarbonyl)acridinium fragment substituted at the benzene moiety.[5e,9,10] A disadvantage of the use of these compounds, however, is their tendency to form nonchemiluminescing "pseudobases" in aqueous basic or neutral media.[1,11,12] In order to minimize this effect, derivatives substituted at the benzene ring have been investigated under a wide range of analytical conditions.[10] There are also other acridinium derivatives substituted at C(9) with carboxamide,[13] cyanide,[2b] and hydroxamic acid or other groups,[5c] whose chemiluminogenic features have been investigated in the context of possible analytical applications.

The stability of acridinium cations functionalized at C(9) and their susceptibility to oxidation depend primarily on the structure of the fragment removed during the formation of electronically excited, N(10)-substituted, 9-acridinones.[1,10,13] The easily removable fragments give rise to flash-type CL, during which the efficiency of light emission is high.[10c,d,12] It has been found that CL efficiency is generally related to the pK_a values of the phenols that are the precursors of N(10)-substituted 9-(phenoxycarbonyl)acridinium cations.[1,13] If these cations are derived from phenols exhibiting a $pK_a < 11.97$ (pK_a of HOOH), they may well turn out to be efficient chemiluminogens.[3,13,14] Unfortunately, however, a higher CL efficiency is usually accompanied by a greater susceptibility to hydrolysis and lower stability of the compounds in aqueous systems. On the other hand, the substituents on the acridinium nucleus affect the wavelength of the emitted light and alter the susceptibility of entities to hydrolysis.[14,15]

The mechanism of oxidation of N(10)-substituted 9-(phenoxycarbonyl)acridinium cations with hydrogen peroxide in alkaline media has been discussed by several authors;[1,3,5c,13] we examined it at the semiempirical level of theory.[4] Computations have shown that the commonly suggested reaction pathway, involving the formation of dioxethanone as intermediate and the elimination of CO_2, is not the most probable means by which light is generated. The results of our studies suggest that light-emitting molecules of 10-methyl-9-acridinone are formed as a result of the elimination of the phenyl carbonate anion, and not CO_2 as other authors have suggested,[1,5c] from the cyclic intermediate that is formed after the initial addition of OOH^- to the 10-methyl-9-(phenoxycarbonyl)acridinium cation and the subsequent abstraction of a proton by OH^-. Analysis of the oxidation of the 9-cyano-10-methylacridinium cation revealed a similar mechanism of CL generation.[16]

This work focuses on experimental and computational investigations of the chemiluminescent features of 10-methyl-9-(phenoxycarbonyl)acridinium cations substituted with various alkyl groups in the phenyl fragment ($MPCA^+$) (Chart 1). By undertaking these investigations we hoped not only to extend our knowledge of practically important chemiluminogens but also to gain an opportunity to study the relations between the physicochemical properties and structure and the chemiluminogenic ability and composition of the reacting systems, which would form a framework for the rational design and analytical use of these acridinium derivatives.

Results and Discussion

Characteristics of the Compounds. Electronic absorption and emission,[17] IR,[18] NMR,[19] thermoanalytical,[20] X-ray,[21,22] and computational[4,17−20,22] methods were employed to determine various features of the compounds investigated. Some other properties are reported below.

There appear to be conspicuous differences between $MPCA^+$ retention times (R_t) (Table 1S, Supporting Information). Cations containing voluminous alkyl substituents or that are

(5) (a) Weeks, I.; Beheshti, I.; McCapra, F.; Campbell, A. K.; Woodhead, J. S. *Clin. Chem.* **1983**, *29*, 1474–1479. (b) Weeks, I.; Sturgess, M.; Brown, R. C.; Woodhead, J. S. *Methods Enzymol.* **1986**, *133*, 366–387. (c) Dodeigne, C.; Thunus, L.; Lejeune, R. *Talanta* **2000**, *51*, 415–439. (d) Kricka, L. J. *Anal. Chim. Acta* **2003**, *500*, 279–286. (e) *Sub-Attomole Labeling Kit*, http://www.assaydesigns.com/objects/catalog/product/extras/915-049.pdf (accessed Oct 1, 2010).

(6) (a) Campos, L. M.; Cavalcanti, C. L.; Lima-Filho, J. L.; Carvalho, L. B.; Beltrao, E. I. *Biomarkers* **2006**, *11*, 480–484. (b) Scorilas, A.; Agiamarnioti, K.; Papadopoulos, K. *Clin. Chim. Acta* **2005**, *357*, 159–167.

(7) (a) Garcia-Campana, A. M.; Baeyens, W. R. G.; Cuadros-Rodriguez, L.; Ales Barrero, F.; Bosque-Sendra, J. M.; Gamiz-Gracia, L. *Curr. Org. Chem.* **2002**, *6*, 1–20. (b) Garcia-Campana, A. M.; Gamiz-Gracia, L.; Baeyens, W. R. G.; Bariero, F. A. *J. Chromatogr. B* **2003**, *793*, 49–74. (c) Atanassova, D.; Kefalas, P.; Psillakis, E. *Environ. Int.* **2005**, *31*, 275–280.

(8) King, D. W.; Cooper, W. J.; Rusak, S. A.; Peake, B. M.; Kiddle, J. J.; O'Sullivan, D. W.; Melamed, M. L.; Morgan, C. R.; Theberge, S. M. *Anal. Chem.* **2007**, *79*, 4169–4176.

(9) (a) Fan, A.; Cao, Z.; Li, H.; Kai, M.; Lu, J. *Anal. Sci.* **2009**, *25*, 587–597. (b) Brown, R. C.; Li, Z.; Rutter, A. J.; Mu, X.; Weeks, O. H.; Smith, K.; Weeks, I. *Org. Biomol. Chem.* **2009**, *7*, 386–394.

(10) (a) Sato, N. *Tetrahedron Lett.* **1996**, *37*, 8519–8522. (b) Razavi, Z.; McCapra, F. *Luminescence* **2000**, *15*, 239−244, 245–249. (c) Smith, K.; Li, Z.; Yang, J.-J.; Weeks, I.; Woodhead, J. S. *J. Photochem. Photobiol. A: Chem.* **2000**, *132*, 181–191. (d) Smith, K.; Yang, J.-J.; Li, Z.; Weeks, I.; Woodhead, J. S. *J. Photochem. Photobiol. A: Chem.* **2009**, *203*, 72–79.

(11) Hammond, P. W.; Wiese, W. A.; Waltrop, A. A.; Nelson, N. C.; Arnold, L. J. *J. Biolumin. Chemilumin.* **1991**, *6*, 35–43.

(12) Kaltenbach, M. S.; Arnold, M. A. *Microchim. Acta* **1992**, *108*, 205–219.

(13) Adamczyk, M.; Mattingly, P. G. In *Luminescence Biotechnology Instruments and Applications* (*Chemiluminescent N-Sulfonylacridinium 9-Carboxamides and Their Application in Clinical Assays*); Van Dyke, K., Van Dyke, C., Woodfork, K., Eds.; CRC Press: Boca Raton, 2002; pp 77−103.

(14) Krzyminski, K.; Roshal, A. D.; Zadykowicz, B.; Bialk-Bielinska, A.; Sieradzan, A. *J. Phys. Chem. A* **2010**, *114*, 10550–10562.

(15) Natrajan, A.; Sharpe, D.; Costello, J.; Jiang, Q. *Anal. Biochem.* **2010**, *406*, 204–213.

(16) Wroblewska, A.; Huta, O. M.; Midyanyj, S. V.; Patsay, I. O.; Rak, J.; Blazejowski, J. *J. Org. Chem.* **2004**, *69*, 1607–1614.

(17) Krzyminski, K.; Roshal, A. D.; Niziolek, A. *Spectrochim. Acta, Part A* **2008**, *70*, 394–402.

(18) Zadykowicz, B.; Ozog, A.; Krzyminski, K. *Spectrochim. Acta, Part A* **2010**, *75*, 1546–1551.

(19) Krzyminski, K.; Malecha, P.; Zadykowicz, B.; Wroblewska, A.; Blazejowski, J. *Spectrochim. Acta, Part A* **2011**, *78*, 401−409.

(20) Krzyminski, K.; Malecha, P.; Storoniak, P.; Zadykowicz, B.; Blazejowski, J. *J. Therm. Anal. Cal.* **2010**, *100*, 207–214.

(21) (a) Sikorski, A.; Krzyminski, K.; Konitz, A.; Blazejowski, J. *Acta Crystallogr., Sect. C* **2005**, *61*, o50–o52. (b) Sikorski, A.; Krzyminski, K.; Bialonska, A.; Lis, T.; Blazejowski, J. *Acta Crystallogr., Sect. E* **2006**, *62*, o555–o558. (c) Sikorski, A.; Krzyminski, K.; Bialonska, A.; Lis, T.; Blazejowski, J. *Acta Crystallogr., Sect. E* **2006**, *62*, o822–o824. (d) Sikorski, A.; Krzyminski, K.; Malecha, P.; Lis, T.; Blazejowski, J. *Acta Crystallogr., Sect. E* **2007**, *63*, o4484–o4485. (e) Trzybinski, D.; Krzyminski, K.; Sikorski, A.; Malecha, P.; Blazejowski, J. *Acta Crystallogr., Sect. E* **2010**, *66*, o826–o827. (f) Trzybinski, D.; Krzyminski, K.; Sikorski, A.; Blazejowski, J. *Acta Crystallogr., Sect. E* **2010**, *66*, o906–o907. (g) Trzybinski, D.; Krzyminski, K.; Sikorski, A.; Blazejowski, J. *Acta Crystallogr., Sect. E* **2010**, *66*, o1311–o1312. (h) Trzybinski, D.; Krzyminski, K.; Blazejowski, J. *Acta Crystallogr., Sect. E* **2010**, *66*, o2773–o2774. (i) Trzybinski, D.; Krzyminski, K.; Blazejowski, J. *Acta Crystallogr., Sect. E* **2010**, *66*, o2929–o2930.

(22) Niziolek, A.; Zadykowicz, B.; Trzybinski, D.; Sikorski, A.; Krzyminski, K.; Blazejowski, J. *J. Mol. Struct.* **2009**, *920*, 231–237.

CHART 1. Canonical Structure of 10-Methyl-9-(phenoxycarbonyl)acridinium Cations Investigated ($MPCA^+$) with the Numbering of Atoms Indicated

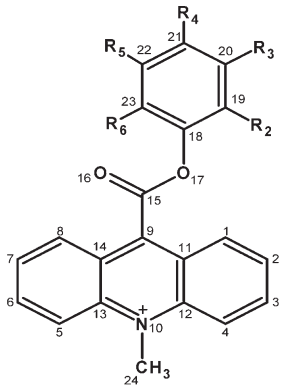

cpd	constitution of the cation					name of the cation
no.	R_2	R_3	R_4	R_5	R_6	
1	H	H	H	H	H	10-methyl-9-(phenoxycarbonyl)acridinium
2	CH_3	H	H	H	H	10-methyl-9-[(2-methylphenoxy)carbonyl]acridinium
3	H	CH_3	H	H	H	10-methyl-9-[(3-methylphenoxy)carbonyl]acridinium
4	H	H	CH_3	H	H	10-methyl-9-[(4-methylphenoxy)carbonyl]acridinium
5	CH_2CH_3	H	H	H	H	9-[(2-ethylphenoxy)carbonyl]-10-methylacridinium
6	$CH(CH_3)_2$	H	H	H	H	9-[(2-iso-propylphenoxy)carbonyl]-10-methylacridinium
7	$C(CH_3)_3$	H	H	H	H	9-[(2-*tert*-butylphenoxy)carbonyl]-10-methylacridinium
8	CH_3	H	H	CH_3	H	9-[(2,5-dimethylphenoxy)carbonyl]-10-methylacridinium
9	CH_3	H	H	H	CH_3	9-[(2,6-dimethylphenoxy)carbonyl]-10-methylacridinium
10	H	CH_3	CH_3	H	H	9-[(3,4-dimethylphenoxy)carbonyl]-10-methylacridinium
11	H	CH_3	H	CH_3	H	9-[(3,5-dimethylphenoxy)carbonyl]-10-methylacridinium
12	CH_3	H	CH_3	H	CH_3	10-methyl-9-[(2,4,6-trimethylphenoxy)carbonyl]acridinium

multiply substituted in the benzene ring exhibit higher t_R values in the reversed-phase system. The R_t values of selected $MPCA^+$ follow the trend of changes in the hydrophobicity parameter (0.56 (Me), 1.02 (Et), 1.53 (*i*-Pr), and 1.98 (*t*-Bu));[23] i.e., they increase in the order **2** < **5** < **6** < **7**. R_t values also tend to increase linearly with increasing values of the base 10 logarithm of the *n*-octanol/water partition coefficient and of the molar refractivity computed using the Biobyte program (Figure 1S, Supporting Information).[24] The similar dependencies noted in other systems follow the general rule that the retention time is proportional to the hydrophobicity of the analyte.[25]

The MS spectra of the compounds investigated are similar. The common signal, always appearing at $m/z = 193$ (Figure 2S, Supporting Information), can be attributed to the cation of the N(10)-methylated acridinium nucleus, which is quite resistant to fragmentation.

General Features of Chemiluminescence. Stationary spectra of the chemiluminescence accompanying the oxidation of selected compounds (**1**, **2**, and **9**) are presented in Figure 3S together with the fluorescence spectrum of 10-methyl-9-acridinone (Supporting Information). In basic aqueous media, CL ranges from 400 to 550 nm, reaching a maximum around 450 nm, like the emission due to the oxidation of other acridinium cations.[2b,26] The emitting entity is 10-methyl-9-acridinone, as emerges from a comparison of experimental spectra and computational predictions for this compound.[14,27] Further support for this conclusion comes from a comparison of the CL and the fluorescence spectra of the oxidation products of **1**, **2**, and **9**. The spectral patterns are almost identical in all cases. This confirms that 10-methyl-9-acridinone is indeed the emitting entity, accounting for the chemiluminescence in the systems investigated.

As CL and fluorescence spectra are broad and exhibit a complex pattern, we measured the emission decay of 10-methyl-9-acridinone dissolved in acetonitrile in order to find out whether it originates from one or more excited forms. Fluorescence decay appears to be monoexponential, which implies that emission comes from only one excited form

(23) Hansch, C.; Leo, A. In *Substituent Constants for Correlation Analysis in Chemistry and Biology*; Wiley: New York, 1979.
(24) BioByte, Inc., Claremont, CA, 1999; available: www.biobyte.com (accessed 1/10/2010).
(25) Paschke, A.; Neitzel, P. L.; Walther, W.; Schuurmann, G. *J. Chem. Eng. Data* **2004**, *49*, 1639–1642.
(26) Cass, M. W.; Rapaport, E.; White, E. H. *J. Am. Chem. Soc.* **1972**, *94*, 3168–3175.
(27) Bouzyk, A.; Jozwiak, L.; Kolendo, A.Yu.; Blazejowski, J. *Spectrochim. Acta, Part A* **2003**, *59*, 543–558.

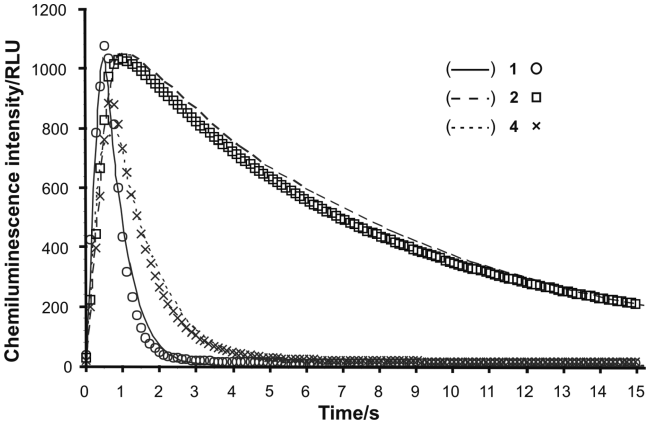

FIGURE 1. Time-dependent chemiluminescence intensity, in relative light units (RLU), profiles for **1**, **2**, and **4** ($c(MPCA^+) = 2 \times 10^{-5}$ M, $c(H_2O_2) = 4.9$ mM, pH = 11.6) (points), together with curves obtained from fitting with eqs 3 and 4.

TABLE 1. Kinetic Data Derived from the Analysis of Time-Dependent Chemiluminescence Profiles[a]

compd no. (Chart 1)	k_1	k_2	t_{max}	C
1	2.49	2.82	0.50	2790
2	2.69	0.119	1.0	1160
3	2.22	2.22	0.62	2670
4	2.41	1.02	0.62	4280
5	2.90	0.068	1.1	3130
6	3.25	0.041	0.93	2280
7	2.90	0.004	22	161
8	3.05	0.095	0.99	871
9	3.81	0.006	16	303
10	2.37	0.893	0.74	7070
11	2.46	1.75	0.62	1960
12	2.71	0.004	2.1	110

[a] k_1 and k_2 (in s^{-1}), t_{max} (in s) and C (in RLU) (eqs 3 and 4) represent mean values from the fitting of at least five replicate time-dependent chemiluminescence intensity profiles (Figure 1); the correlation coefficient for the fitting of an individual profile was better than 0.95.

(Figure 4S, Supporting Information). The average fluorescence lifetime was found to be 6.6×10^{-9}s.

Kinetic Features of Chemiluminescence. Chemiluminescence intensity always grows, reaches a maximum, and falls in time. The fitting of time-dependent CL profiles, an example of which is given in Figure 1, with eqs 3 and 4 for two-step consecutive chemical processes yields the kinetic characteristics shown in Table 1. Values of k_1, reflecting CL growth, vary between 2.2 and 3.9 s^{-1}. They account for the competitive reaction of OOH^- or OH^- with $MPCA^+$ and also for the diffusion processes involving these entities, which are difficult to quantify in kinetic analysis. Furthermore, the relatively small number of points harvested in the initial region of the CL−time profiles causes uncertainties in the evaluation of k_1. For these reasons, k_1 seems to be less suitable for an in-depth analysis.

Values of k_2, reflecting chemiluminescence decay, are more widely differentiated than k_1 (Table 1). The lowest k_2 characterizes the drop in chemiluminescence in **7** and **12**, the highest, in **1**. If $k_2 > 1$ s^{-1}, flash-type chemiluminescence occurs. When k_2 values are low, long-lasting (glow-type) chemiluminescence is observed.[9b,10c,d] The data in Table 1 indicate that there is an approximately inverse relationship between k_2 and t_{max} (eq 4). Low t_{max} values correspond to

TABLE 2. Physicochemical Characteristics of Chemiluminescence Accompanying the Reaction of $MPCA^+$ with OOH^- in Alkaline Aqueous Media

		relative CL efficiency at various pH[b] (%)		
compd no. (Chart 1)	$CQY^a \times 10^{-2}$	12.0	10.0	8.0
1	1.88	100.0	87.0	6.48
2	1.60	85.0	39.5	0.86
3	1.88	100.3	84.4	5.16
4	1.71	91.2	73.5	2.40
5	1.31	70.0	13.9	0.56
6	1.08	57.3	10.1	0.34
7	0.63	33.5	4.5	1.11
8	1.22	65.2	22.6	0.39
9	1.12	59.9	7.3	0.42
10	1.49	79.4	59.3	1.32
11	2.21	117.6	94.6	4.01
12	0.59	31.4	9.2	5.45

[a] Mean values (in einstein/mol) of five replicate measurements ($c(MPCA^+) = 2 \times 10^{-8}$ M, $c(H_2O_2) = 4.9$ mM, pH = 11.6) obtained using luminol as a standard[28] (the coefficient of variability varied between 0.02 and 0.08). [b] Values obtained from the formula 100% × light sum of **2**−**12** (pH = 8.0, 10.0 and 12.0)/light sum of **1** (pH = 11.6, $c(MCPA^+) = 2 \times 10^{-5}$ M, $c(H_2O_2) = 4.9$ mM).

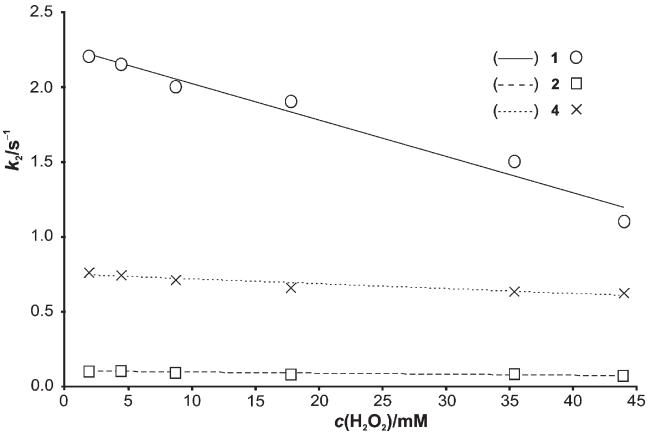

FIGURE 2. Dependence of k_2 on H_2O_2 concentration for **1**, **2**, and **4** ($c(MPCA^+) = 2 \times 10^{-8}$ M, pH = 11.6) (points), together with lines resulting from least-squares fitting.

cases of flash-type chemiluminescence. Values of C (eq 3) are qualitatively related to the CL efficiency/chemiluminescence quantum yield (Table 2) and can thus be considered as a measure of the probability that $MPCA^+$ will be converted to light emitting species.

A set of k_1, k_2, t_{max}, and C reflects the chemiluminogenic features and is characteristic of a given $MPCA^+$. CL is quite weak in the case of **6**, **7**, **9**, and **12**, i.e., when bulky (*i*-Pr and *t*-Bu) substituents (**6** and **7**) or two Me substituents (**9** and **12**) are in the *ortho* position of the benzene ring. Values of k_2 in the series of **2**, **5**, **6**, and **7** fall with a decrease in Taft's size parameter, which characterizes the steric effects of the substituents Me, Et, *i*-Pr, and *t*-Bu in the *ortho* position of the benzene ring (respectively equal to −1.24, −1.31, −1.71, and −2.78),[23] and rise with an increase in Charlton's size constant (respectively equal to 0.52, 0.56, 0.76, and 1.24).[23]

Values of k_2 decrease linearly with increasing H_2O_2 concentration, which is shown for selected compounds in Figure 2. The slopes of these dependencies, respectively, equal to 31.1,

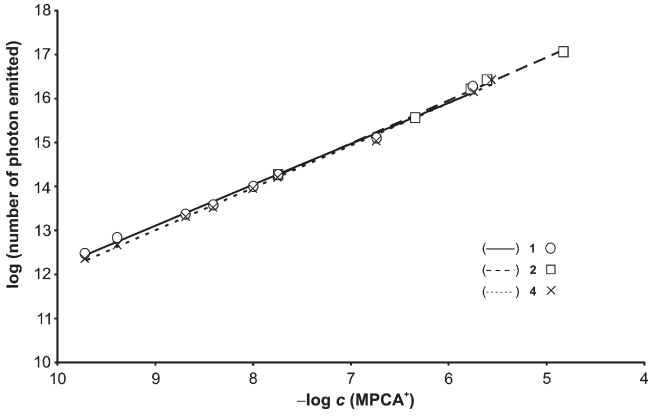

FIGURE 3. Number of photons emitted from 1 mol of $MPCA^+$ (n.p.) versus concentration of **1**, **2**, and **4** ($c(H_2O_2)$ = 4.9 mM, pH = 11.6). Lines correspond to the following equations: n.p. = $1.16 \times 10^{22} \times c(MPCA^+)$ (**1**), n.p. = $9.03 \times 10^{21} \times c(MPCA^+)$ (**2**), n.p. = $1.13 \times 10^{22} \times c(MPCA^+)$ (**4**).

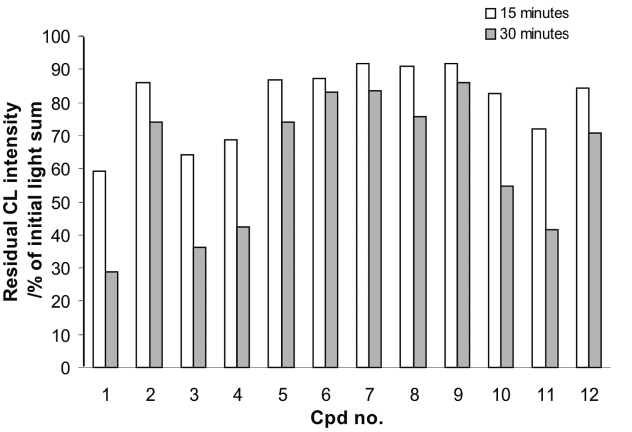

FIGURE 4. Stability of $MPCA^+$ ($c = 2 \times 10^{-5}$ M) over time in basic medium ($c(H_2O_2)$ = 4.9 mM, pH = 8.0).

1.23, and 4.56 M^{-1} s^{-1} for **1**, **2**, and **4**, reflect the overall processes in which $MPCA^+$ participates and which do or do not lead to chemiluminescence. A quantitative measure of chemiluminescence is the light sum, the area under the CL−time profile. Light sums/chemiluminescence quantum yields gradually decrease with H_2O_2 concentration (Figures 5S and 6S, Supporting Information), which raises the problem of the choice of the appropriate value of this quantity in chemiluminogenic assays. At pH 11.6, the value assumed in assays using acridinium chemiluminogens,[10] about half the H_2O_2 molecules (pK_a = 11.97), are in anionic (OOH^-) form. In all experiments, therefore, there is a large excess (several orders of magnitude) of OOH^- over $MPCA^+$. Lowering the H_2O_2 concentration leads to an increase in the light sums, as mentioned above. However, at H_2O_2 concentrations lower than 0.5 mM, the reproducibility of the assays deteriorates. Thus, an H_2O_2 concentration equal to 4.9 mM was assumed to be optimal in our investigations.

Chemiluminescence Quantum Yields. The plots of the total number of photons emitted (light output) against $MPCA^+$ concentration are linear over a wide range of concentrations, as in the case of other acridinium chemiluminogens.[1c,5e] This indicates that the compounds investigated can be used as chemiluminescent indicators. The calibration graphs for **1**, **2**, and **4** are presented by way of example in Figure 3. The slopes of these graphs are, respectively, equal 1.13×10^{22} (**1**), 9.61×10^{21} (**2**), and 1.03×10^{22} (**4**) and represent the total number of photons emitted from 1 mol of $MPCA^+$. This information enables one to obtain the chemiluminescence quantum yields (CQY), given in Table 2, using luminol as a reference system. The lowest measurable light output reflects the detection limit of $MPCA^+$. The minimum detectable concentration of the compounds investigated at pH = 11.6 is in the 10^{-10} M range. Compounds exhibiting flash-type chemiluminescence are generally more readily detectable (lower mdc) than chemiluminogens showing glow-type chemiluminescence (higher mdc).

Quantum yields (Table 2) directly reflecting the tendency of $MPCA^+$ to chemiluminesce lie in the range 0.59×10^{-2} − 2.21×10^{-2} einstein/mol (CQY for luminol = 1.23×10^{-2} einstein/mol);[28] *meta*-substituted (**11** and **3**) and unsubstituted (**1**) compounds have the highest values. Values of CQY decrease with increasing size of the *ortho* substituent in the benzene ring (in the order **2** > **5** > **6** > **7**) or when two Me substituents are present in the *ortho* position (**9** and **12**). If Me is in the *para* position (**4**), there is a slight decrease in CQY compared to the unsubstituted compound (**1**). A rise in pH from 8.0 to 12.0 substantially increases CQY (Table 2). The interrelations between CQYs are similar at various pH, which means that structural factors affect the chemiluminogenic ability of $MPCA^+$ in a similar way as the basicity of the medium changes.

Stability of $MPCA^+$ in Basic Media. $MPCA^+$ lose 8−40% of their initial chemiluminogenic ability after 15 min of thermostatting and 14−70% after 30 min of thermostatting at pH = 8.0 (Figure 4). The chemiluminogenic ability of **1** falls most distinctly in time. All other cations substituted at the benzene ring are more resistant to the influence of alkaline media and the decrease of chemiluminogenic ability. The resistance of $MPCA^+$ to alkaline media increases slightly with the size of the substituent in the *ortho* position, i.e., on the order **2** < **5** < **6** < **7**. The resistance is the greatest if two Me substituents are present in the *ortho* position (**9**). *Meta*-substituted derivatives (**3** and **11**) are only slightly more resistant to alkaline hydrolysis than the unsubstituted compound (**1**). Compound **12**, containing two Me substituents in the *ortho* position and one Me in the *para* position, exhibits a lower resistance to alkaline media than **9**, which has only two Me substituents in the *ortho* position.

The above findings may indicate the site to which $MPCA^+$ should be attached to investigate or assay macromolecules. Usually, the links are via a spacer and an active group to the *para* position of the benzene ring,[5e] although the resistance to hydrolysis of a tracer or label should be improved if *ortho* positions are used for connecting the side arm.[10d]

The results of our investigations concerning the stability of $MPCA^+$ in basic media follow the trends reported so far,[10a,d] but the values of the relevant properties are generally lower in our case (Table 2). On the other hand, the stability of $MPCA^+$ was investigated mostly in acidic aqueous media, the environment in which tracers are stored prior to analytical use.

The question arises as to how aqueous alkaline media influence the stability of $MPCA^+$ and, consequently, their chemiluminogenic ability. It is thought that C(9) is susceptible

(28) Ando, Y.; Niwa, K.; Yamada, N.; Irie, T.; Enomoto, T.; Kubota, H.; Ohmiya, Y.; Akiyama, H. *Photochem. Photobiol.* **2007**, *83*, 1205–1210.

to nucleophilic substitution simultaneously by OOH^- (the form of H_2O_2 existing in alkaline media) and OH^- (pH > 7.0).[1b,4,13,16] In the former case, an intermediate is formed that is subsequently converted to electronically excited light emitting 10-methyl-9-acridinone. In the latter case, a so-called "pseudobase" is formed,[1,4,13] which is not converted to a light emitting species. The introduction of $MPCA^+$ to alkaline media would thus bring about the formation of the relevant "pseudobases", which cannot be converted to the products of the addition of OOH^- to $MPCA^+$ because the activation barrier for this process is quite high.[2b] For these reasons, $MPCA^+$ and H_2O_2 are mixed in acidic conditions, and chemiluminescence is triggered by the addition of the aqueous base solution. In such a situation, OH^- and OOH^- appear simultaneously and compete for the cation according to the rules of probability of encountering reacting entities, since both processes proceed in the absence of activation barriers.[4,16] Therefore, the loss of the chemiluminogenic ability of $MPCA^+$ in alkaline media is caused predominantly by "pseudobase" formation and its subsequent transformation to nonexcited molecules of 10-methyl-9-acridinone.[1a,5c]

Another possible reason for the loss of chemiluminogenic ability is the partial alkaline hydrolysis of $MPCA^+$, resulting from the attack of OH^- and/or OOH^- on the carbonyl C(15) atom (Chart 1), leading to the production of nonchemiluminogenic 9-carboxy-10-methylacridinium acid.[9b,13,14]

Origin of Chemiluminescence. According to the mechanisms of the oxidation of 10-methylacridinium derivatives by H_2O_2 in alkaline media put forward in the literature,[1,4,5c,13] the primary steps are determined mainly by the location of the electrophilic center in the cation. As indicated by frontier orbital theory,[29] the LUMO distribution in an electrophilic species (cations) determines the molecular centers sensitive to nucleophilic attack of OOH^- or OH^-. The LCAO coefficients of the p_z $MPCA^+$'s LUMO is ca. 10 times higher at the endocyclic C(9) than at the carbonyl group C(15) atom (0.325 and 0.04, respectively; average for **1**, **4**, **7**, and **12**).[19] This implies that C(9) rather than the C(15) atom of the carbonyl group is the site of the primary nucleophilic attack of the above-mentioned anions, despite the fact that the electronic charge deficiency at C(9) is lower than at C(15) (Mulliken relative partial charges are 0.09 and 0.51, respectively; average for **1**, **4**, **7**, and **12**).[19]

Another factor important for the generation of chemiluminescence is that H_2O_2 reacts spontaneously with OH^- yielding OOH^-.[1b,4,13,16]

Taking into account the mechanisms of the chemiluminescence of 10-methylacridinium cations proposed in the literature,[1,5c] and following our findings so far,[4,16] we considered only certain processes, which are shown in Scheme 1. These processes account for the chemiluminescence (steps I, V, and VI), the formation of the so-called "pseudobase" (step II), and the appearance of phenoxy anions (steps VII; II, VIII and IX or II, X and XI; and IV and XIV) and 10-methylacridinium-9-carboxylate anions (steps IV and XIV) among the reaction products. All of the primary steps I−IV proceed spontaneously since they are reactions between ions (Table 3). Which intermediate (**16**, **23**, **28**, or **29**) occurs depends on the thermodynamic factors preferred in step II and on the kinetic preferences, which seem to be similar for steps I−IV. In this way, a certain amount of intermediate **16**, identified experimentally,[13,14] is formed, which is the precursor of the light-emitting species. The possible simultaneous occurrence of steps I−IV lessens, however, the probability of the formation of **16** and consequently the efficiency of CL. Moreover, **23** would be difficult to convert to **16** by S_N2 substitution with OOH^- and likewise **16** to **23** by S_N2 substitution with OH^-, owing to the expected relatively high activation barrier to such processes.[2b] Thus, once **16** is produced, it reacts immediately with OH^- to form the cyclic intermediate **17**, which then decomposes to the energy-rich 10-methyl-9-acridinone (**19**) and phenyl carbonate anion (**20**) (Table 3). The energy released in step VI (Table 3) exceeds that necessary to cause electronic excitation of 10-methyl-9-acridinone (88.2 kcal/mol).[27] Hence, the excited 10-methyl-9-acridinone molecules emit light, which is manifested as CL. Electronically excited molecules of 10-methyl-9-acridinone could also be formed via steps III, XIII, and VI. The latter pathway is, however, less probable than that via steps I, V, and VI, since the thermodynamic force ($\Delta_{r,298}G^o$) for step III is lower than that for step I (Table 3) and the probability of nucleophilic substitution of OOH^- at the carbonyl C(15) atom is much lower than at C(9), as indicated by the values of the p_z LUMO. It has long been assumed that the formation of electronically excited 10-methyl-9-acridinone is accompanied by the release of phenoxy anions from **17** and the subsequent elimination of CO_2 from the intermediate thus formed (10-methyl-10*H*-spiro[acridine-9,3′-[1,2]dioxetane]-4′-one (**31**) (Figure 6S, Supporting Information)).[1,5c] We found previously, however, that such processes need to overcome quite high activation barriers.[4] The barriers predicted for the latter process, **31** → **19** + **22**, are respectively ($\Delta_{a,298}H^o$ (gaseous phase), $\Delta_{a,298}G^o$ (gaseous phase), $\Delta_{a,298}G^o$ (aqueous phase)) equal to (in kcal/mol) 14.3, 14.9, and 15.9. They thus remain relatively high, which suggests that the formation of electrically excited molecules of 10-methyl-9-acridinone proceeds via the elimination of phenyl carbonate anions rather than the consecutive release of phenoxy anions and CO_2. Phenyl carbonate anions do not decompose instantaneously to CO_2 and phenoxy anions in alkaline media in reactions leading to chemiluminescence (step VII) (Table 3). In acidic media, however, in which reaction products were identified, the former ions can be decarboxylated, as will be shown later, to form the corresponding phenols, which were identified together with the ones produced via steps IX, XI, or XIV (**27** and **30** have been regarded as byproducts of the oxidation of 10-methyl-9-(phenoxycarbonyl)-acridinium cations in alkaline media).[1,9b,14,26] The evidence for the above mechanism would undoubtedly be strengthened by the identification of phenyl carbonate anions. We have been tackling this problem.

Reactions between ionic species (steps I−IV) and proton abstraction by OH^- (steps V, VIII, XIII, and XIV) exhibit low activation barriers, if any. Thus, the processes in which such barriers can be expected are steps VI and IX−XII. The predicted barriers for step VI are moderate, which means that elimination of phenyl carbonate anions and the formation of electronically excited 10-methyl-9-acridinone molecules is achieved under the experimental conditions applied (Table 4). This also confirms the predicted quite high rate constants and low reaction completion times. It should,

(29) Fleming, I. *Frontier Orbitals and Organic Chemical Reactions*; Wiley: London, 1976.

SCHEME 1. Pathways of the Reactions of $MPCA^+$ with OOH^- and OH^-

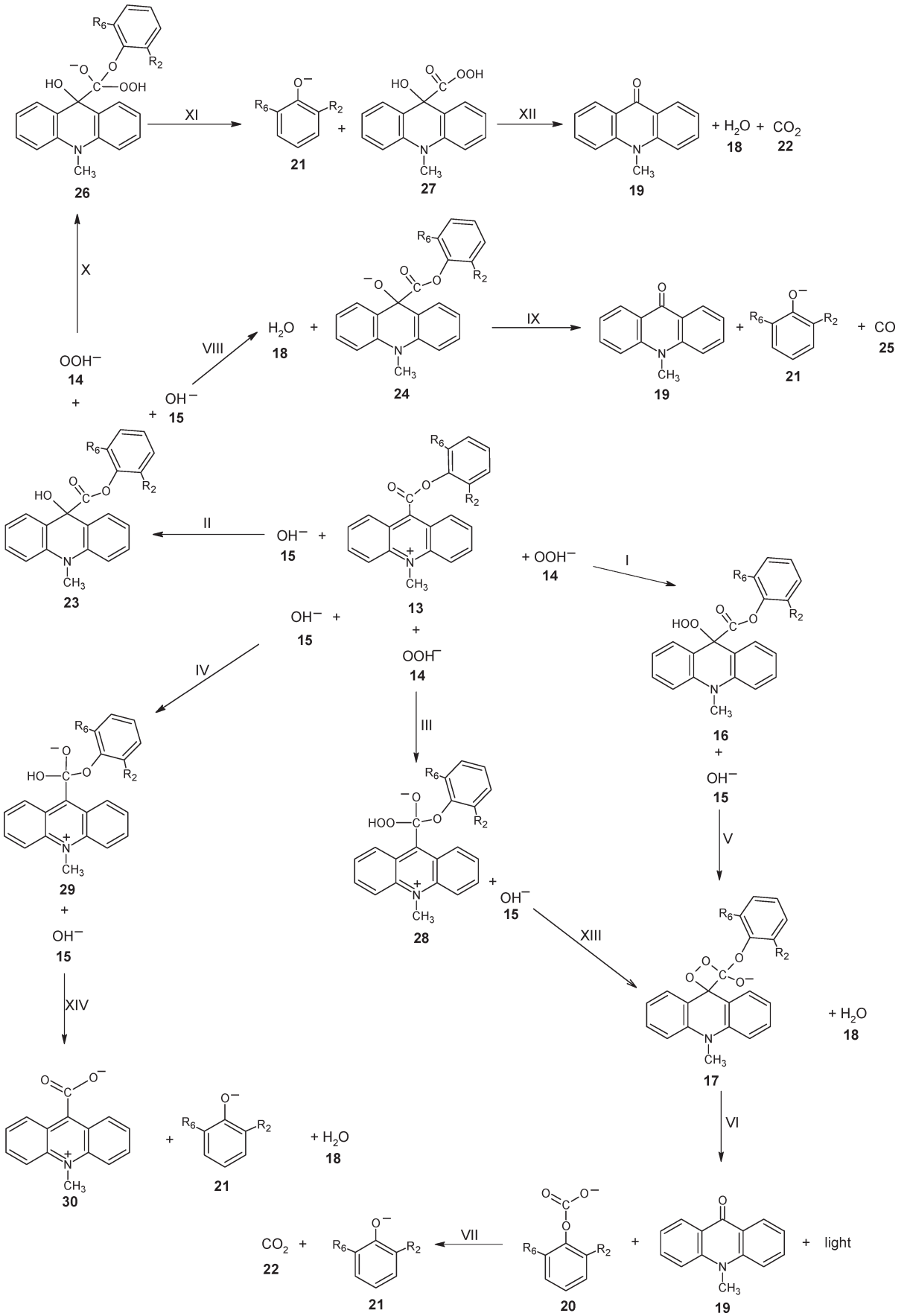

however, be noted that Gibbs' free energies of activation (Table 4) do not account for the trends revealed by analysis of chemiluminescence quantum yields (Table 2); **1** and **2** exhibit relatively high Gibbs' free energy activation barriers and relatively high CQY, and **9** exhibits a low activation barrier and low CQY, but the expected tendency should be the opposite. Therefore, DFT computations suggest that factors other than kinetic ones may determine the efficiency of chemiluminescence. The formation of "pseudobase" (**23**) initiates nonchemiluminescent pathways of $MPCA^+$ depletion. According to our predictions, the activation barriers to steps X and XI, i.e., the substitution at OOH^- of the carbonyl C atom of **23** and the release of the phenoxy anion from the entity thus formed, appear to be less than 0.1 kcal/mol each. Activation barriers do, however, exist for the final steps (IX and XII) of the dark transformation of $MPCA^+$ to 10-methyl-9-acridinone (Table 4), but the energy released in the latter two processes is too small (Table 3) to electronically excite the above product. The activation barriers to steps IX and XII, responsible for the dark transformation of $MPCA^+$ to 10-methyl-9-acridinone, are higher than that of step VI; the former steps should thus be slower than the latter one. Nevertheless, they may occur, and when they do, they cause irreversible loss of the chemiluminogenic ability of $MPCA^+$.

TABLE 3. Thermodynamic Data (in kcal/mol) of the Elementary Steps of the Reactions of 1, 2, and 9 with OOH^- and OH^- [a]

		gaseous phase		aqueous phase
step no. (Scheme 1)	compd no.	$\Delta_{r,298}H°$	$\Delta_{r,298}G°$	$\Delta_{r,298}G°$
I	**1**	−166.6	−153.6	−51.5
	2	−167.6	−155.0	−51.6
	9	−167.9	−155.3	−53.3
II	**1**	−186.1	−175.6	−73.3
	2	−193.6	−182.7	−74.4
	9	−194.0	−183.9	−74.4
III	**1**	−139.1	−125.3	−33.1
	2	−133.6	−120.4	−26.7
	9	−132.7	−118.9	−27.8
IV	**1**	−157.9	−147.1	−55.2
	2	−158.7	−148.6	−55.9
	9	−157.0	−146.7	−48.3
V	**1**	−75.2	−75.6	−37.7
	2	−74.9	−75.3	−38.3
	9	−72.9	−72.7	−35.6
VI	**1**	−94.1	−108.3	−105.2
	2	−94.4	−108.6	−104.4
	9	−95.4	−110.2	−105.6
VII	**1**	14.4	7.0	14.1
	2	13.3	5.9	13.9
	9	11.3	3.3	14.8
VIII	**1**	−72.9	−73.1	−32.1
	2	−66.2	−67.4	−27.0
	9	−67.4	−67.3	−28.4
IX	**1**	3.4	−20.8	−6.1
	2	2.2	−22.1	−7.1
	9	2.4	−22.9	−4.0
X	**1**	−67.0	−53.0	−24.1
	2	−59.5	−45.8	−20.8
	9	−54.0	−38.4	−15.2
XI	**1**	16.1	1.2	1.2
	2	14.0	−1.5	2.0
	9	7.5	−9.5	−1.9
XII		−84.4	−103.0	−87.2
XIII	**1**	−102.6	−103.9	−56.2
	2	−108.8	−109.9	−62.9
	9	−108.2	−109.0	−61.0
XIV	**1**	−84.3	−98.8	−58.2
	2	−85.6	−99.8	−57.6
	9	−88.7	−103.6	−64.5

[a] $\Delta_{r,298}H°$ and $\Delta_{r,298}G°$, respectively, represent the enthalpy and Gibbs' free energy (gaseous phase) or free energy (aqueous phase) of the reaction corresponding to a given step number at temperature 298.15 K and standard pressure.

Scheme 1 depicts chemical processes which may or may not lead to chemiluminescence. It does not show, however, how the released energy can be converted to electronic excitation. There are numerous reports suggesting that the decomposition of acridinium 1,2-dioxetanes is accompanied by intramolecular chemically initiated electron exchange luminescence (CIEEL) arising from the electronically excited 10-methyl-9-acridinones formed in the process.[30] There are grounds for believing that such a mechanism may also account for the chemiluminescence generated during the oxidation of 10-methyl-9-(phenoxycarbonyl)acridinium cations in alkaline media.

According to the proposed chemiluminogenic pathway (steps I, V, and VI in Scheme 1), the efficiency of emission should rise with increasing OOH^- concentration, since the latter entity takes part in bimolecular step I. However, the dependencies shown in Figures 5S and 6S (Supporting Information) demonstrate the reverse trend, namely, the decrease in chemiluminescence efficiency with increasing OOH^- concentration. A possible explanation for this finding is that as the concentration of the latter entity increases, so does the contribution of the parallel dark pathway (depicted by steps II, X, XI, and XII in Scheme 1) in the total consumption of the chemiluminogenic precursor (**13**). Such an effect could also explain the drop in k_2 values with increasing OOH^- concentration (Figure 2).

The structures of selected $MPCA^+$ and the entities shown in Scheme 1 and mentioned in the text are presented in the Supporting Information (Figure 6S) to give an idea of the

TABLE 4. Kinetic Characteristics of the Elementary Steps of the Reaction of 1, 2, and 9 with OOH^- and OH^- [a]

		gaseous phase			aqueous phase
step no. (Scheme 1)	compd no.	$\Delta_{a,298}H°$	$\Delta_{a,298}G°$	${}_{298}k°$ (${}_{298}\tau°_{99}$)	$\Delta_{a,298}G°$
VI	**1**	11.8	11.7	4.4×10^4 (1.0×10^{-4})	7.9
	2	11.7	11.4	2.9×10^4 (1.6×10^{-4})	7.9
	9	8.9	8.4	3.8×10^6 (1.2×10^{-6})	2.9
IX	**1**	10.3	7.8	1.3×10^7 (3.7×10^{-7})	14.6
	2	10.0	7.9	1.1×10^7 (4.4×10^{-7})	12.7
	9	11.0	7.8	1.2×10^7 (3.8×10^{-7})	17.1
XII		28.4	30.2	4.2×10^{-10} (1.1×10^{10})	25.2

[a] $\Delta_{a,298}H°$ and $\Delta_{a,298}G°$ (both in kcal/mol), respectively, represent the enthalpy and Gibbs' free energy (gaseous phase) or free energy (aqueous phase) of activation at temperature 298.15 K and standard pressure. ${}_{298}k°$ (in s^{-1}) and ${}_{298}\tau°_{99}$ (in s) (eqs 5 and 6), respectively, denote the rate constant and the time after which the reaction is 99% complete.

molecular transformations taking place along the reaction pathway. The Cartesian coordinates, total energies, and the latter quantity plus the zero point energy, thermal energy/enthalpy, and entropy at 298.15 K and standard pressure, for all the entities appearing in Scheme 1 and the text, and corresponding to stationary (lowest energy and transition state) structures, are given in the Supporting Information.

Products of Processes Leading to Chemiluminescence and Side Processes. Attempts were made to identify some stable and intermediate products of the processes depicted in Scheme 1. Stable products, i.e., 10-methyl-9-acridinone, 9-carboxy-10-methylacridinium acid, and substituted phenols, were found in the acidified reactant mixture after triggering reactions leading to chemiluminescence in **1**, **2**, and **9**. These entities were identified using HPLC with UV absorption detection by adding relevant standards to the reactant mixtures and comparing the retention times of products and standards. The results of selected HPLC analyses are given in Figure 8S and Table 2S (Supporting Information), demonstrating some quantitative data for the identified reaction products. The dominant product was 10-methyl-9-acridinone, whose amount, relative to the initial amount of $MPCA^+$, was 85−96 mol % in postreaction mixtures in the cases of **1** and **2**. The amount of 9-carboxy-10-methylacridinium acid accounts for the depletion of 4−15 mol % of $MPCA^+$. This product is most probably formed as a result of the hydrolysis of $MPCA^+$ (steps IV and XIV in Scheme 1). Lastly, the amount of the corresponding phenols accounts for roughly 100% of $MPCA^+$ depleted in the case of **1** and **2**. Since the HPLC signals of 10-methyl-9-acridinone and phenol in the case of **9** overlapped, it was not possible to estimate the amounts of these products relative to the substrate. The above data demonstrate that $MPCA^+$ undergoes hydrolysis to nonchemiluminescent 9-carboxy-10-methylacridinium acid and that the extent of this process grows with time under the analytical conditions applied. Further, 10-methyl-9-acridinone appears in only somewhat smaller amounts in relation to $MPCA^+$. Since chemiluminescence quantum yields are of the order of a few percent, this product must be formed mainly via nonchemiluminescent chemical and physical pathways, among which is the transformation of "pseudobase" (**23**) to nonexcited 10-methyl-9-acridinone (steps II, VIII−XII in Scheme 1). Lastly, since phenols and depleted $MPCA^+$ were found in roughly equimolar amounts, it seems that they are the products of the chemiluminescent and nonchemiluminescent pathways of the conversion of $MPCA^+$ to 10-methyl-9-acridinone.

The identification of the corresponding phenols does not solve the question whether they are released upon conversion of $MPCA^+$ to 10-methyl-9-acridinone or 9-carboxy-10-methylacridinium acid, or during the decomposition of the phenyl carbonate anions postulated in the chemiluminescence mechanism (steps I, V, and VI in Scheme 1). The latter anions are converted to the corresponding phenyl carbonates under the acidic conditions in which the HPLC analyses were performed and decompose readily to phenols and CO_2 (calculated $\Delta_{r,298}H^o$ (gaseous phase), $\Delta_{r,298}G^o$ (gaseous phase) and $\Delta_{r,298}G^o$ (aqueous phase) are, respectively, equal to (in kcal/mol) −7.1, −15.3, and −4.3 (R_2 = H, R_6 = H); −7.4, −15.6, and −4.8 (R_2 = CH_3, R_6 = H); −7.6, −16.0, and −5.0 (R_2 = CH_3, R_6 = CH_3)). The method used is thus unable to show that phenyl carbonate anions are released in the last step of the reactions leading to the chemiluminescence of $MPCA^+$.

The lack of $MPCA^+$ signals in HPLC analyses and the balance of reactants indicate that all of the substrate is converted to products. Since only a small portion of $MPCA^+$ is converted to light-emitting 10-methyl-9-acridinone, the main part must take part in nonchemiluminescent pathways, among which the one initiated by the attack of OH^- on the electrophilic center of $MPCA^+$ at C(9) leading to the formation of "pseudobase" (**23**) (step II in Scheme 1) seems to dominate. Two pathways are postulated to account for the dark transformation of **23** to 10-methyl-9-acridinone: one via steps VIII and IX and the other one via steps X, XI, and XII. McCapra found that the dark transformation of $MPCA^+$ took place efficiently in the presence of oxidants and postulated **27** as an intermediate.[1a,5c] We also noted that in the absence of oxidants, the "pseudobase" could be converted to $MPCA^+$, but not in their presence, i.e., under the conditions of our chemiluminescence experiments. Steps X, XI, and XII in Scheme 1 offer reasonable support for these findings. On the other hand, the results of computations indicate that **23** may well be transformed to nonexcited 10-methyl-9-acridinone via steps VIII and IX, especially as the latter is kinetically preferred to step XII, since it needs to overcome a lower activation barrier. In this situation, both the above pathways may account for the dark transformation of $MPCA^+$.

In the search for further evidence in support of the assumed reaction scheme, we attempted to detect species **23** ("pseudobase") by carrying out the spectrophotometric acid−base titration of **1**, **2**, and **9**. From the results obtained (Figure 9S, Supporting Information), pK values reflecting the equilibrium $MPCA^+ + OH^- \leftrightarrow$ MPCAOH, equal to −4.73, −4.74, and −4.62 for **1**, **2**, and **9**, respectively, were calculated. Spectrophotometric data reveal that cations of **1**, **2**, and **9** absorb around 260 and 360 nm in acidic media. When the pH increases from 2 to 12 a new maximum appears at 283 nm, which can be ascribed to the "pseudobase". Two isosbestic points characterize the titration profiles, one at 268 nm and the other at 335 nm. At pH = 11.6, at which the chemiluminescence experiments were done, almost all $MPCA^+$ should be in the "pseudobase" form under equilibrium conditions. This means that upon alkalization of the reaction mixture (final step of experiments), the instantaneously occurring OOH^- and OH^- compete for the electrophilic center at C(9) of $MPCA^+$. This competition is one of the crucial factors influencing chemiluminescence quantum yields.

Another pathway competing with chemiluminescence is hydrolysis of $MPCA^+$, the extent of which for **1**, **2**, and **9** is presented in Figure 5. Compound **9**, exhibiting glow-type chemiluminescence, is much more resistant to hydrolysis than **1** and **2**. Two stages of hydrolysis are seen in the case of **1** and **2** (**1** exhibits flash type chemiluminescence), the first, lasting ca. 7 and 25 s, respectively, and the second proceeding several times more slowly. As chemiluminescence in **1** and **2** lasts from 3 to 30 s, respectively, it must be influenced by hydrolysis. The data obtained suggest that from several to a dozen or so percent of $MPCA^+$ are depleted in such a process. Hydrolysis of $MPCA^+$ is initiated by the attack of

(30) Ciscato, L. F. M. L.; Bartoloni, F. H.; Weiss, D.; Beckert, R.; Baader, W. J. *J. Org. Chem.* **2010**, *75*, 6574–6580.

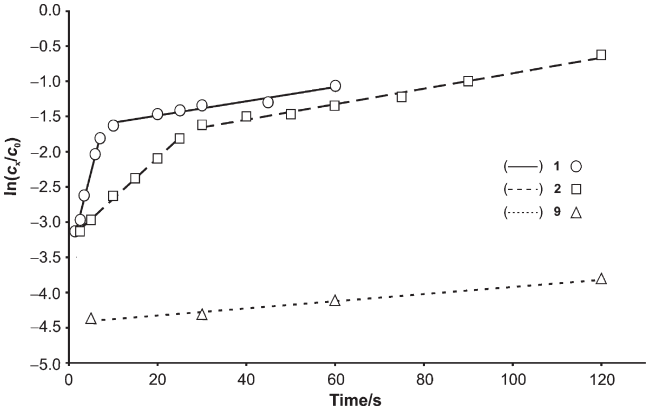

FIGURE 5. Extent of hydrolysis of **1**, **2**, and **9** ($c = 8.3 \times 10^{-4}$ M) at pH = 12.0. The lines correspond to the following equations: (**1**) $\ln(c_x/c_0) = 0.261(t) - 3.55$ (first stage), $\ln(c_x/c_0) = 0.0108(t) - 1.57$ (second stage); (**2**) $\ln(c_x/c_0) = 0.0545(t) - 3.18$ (first stage), $\ln(c_x/c_0) = 0.0145(t) - 2.12$ (second stage); and (**9**) $\ln(c_x/c_0) = 0.0046(t) - 4.41$; c_x and c_0 denote the actual concentration of 9-carboxy-10-methylacridinium acid and the initial concentration of $MPCA^+$, respectively.

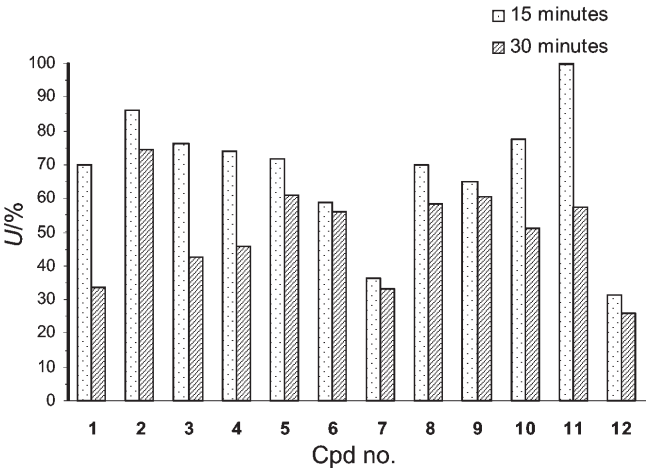

FIGURE 6. Usefulness (U) of $MPCA^+$, the product of residual CL intensity after 15 or 30 min of thermostatting (percent of initial light sum, Figure 4) and relative CL efficiency (percent for pH = 12.0, Table 2), normalized, in %, to the highest value.

OH^- on the C(15) atom of the carboxy group (step IV in Scheme 1). This process competes with steps I, II, and III leading to chemiluminescence and to the dark transformation of the cation to nonemitting 10-methyl-9-acridinone. It is thus possible that this competition has the main influence on the formation 9-carboxy-10-methylacridinium acid.

The Choice of Optimal Chemiluminescent Derivatives. The usefulness of $MPCA^+$ (U) was analyzed (Figure 6) by comparing the products of their relative chemiluminescence efficiency (measured at pH = 12.0) (Table 2) and residual CL intensity after thermostating in alkaline media (pH = 8.0) (Figure 4). At pH = 8.0, chemiluminescent labeling of macromolecules is usually carried out, whereas at about pH = 12 chemiluminescence is initiated.[1,5] The most promising chemiluminescent indicators or fragments of chemiluminescent labels are **2**, **8**, and **9**, i.e., $MPCA^+$ with one or two Me groups in the *ortho* position of the benzene ring, since their CL efficiency is

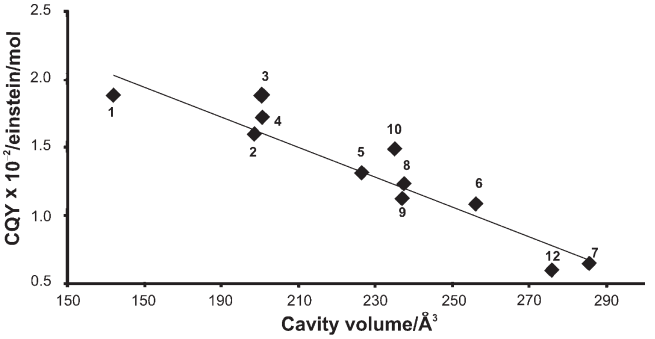

FIGURE 7. Chemiluminescence quantum yields (CQY) (Table 3) against the cavity volume (the volume of the hydration layer) of the respective phenyl carbonate anions (**20** in Scheme 1). The numbers indicate the entities listed in Chart 1; the line corresponds to the equation: CQY = −0.0110 × (cavity volume) + 3.80.

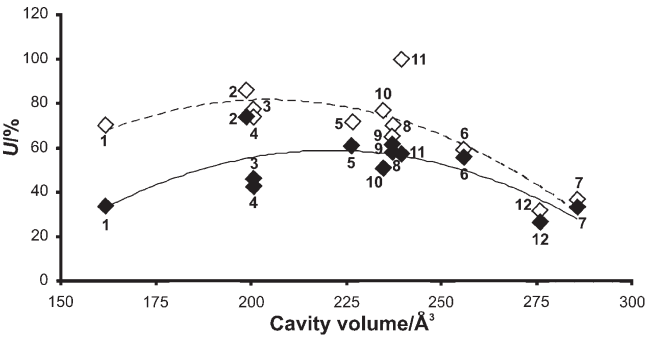

FIGURE 8. Usefulness (U) (Figure 6) against the cavity volume (the volume of the hydration layer) of the respective phenyl carbonate anions (**20** in Scheme 1). Upper graph (empty squares), values corresponding to 15 min of thermostatting; lower graph (filled squares), values corresponding to 30 min of thermostatting. The numbers indicate the compounds investigated (Chart 1); the curves correspond to the equations: $U = -0.00770 \times (\text{cavity volume})^2 + 3.15 \times (\text{cavity volume}) - 240.9$ (upper graph) and $U = -0.00737 \times (\text{cavity volume})^2 + 3.26 \times (\text{cavity volume}) - 301.4$ (lower graph).

relatively high and at the same time they do not lose their chemiluminogenic ability in alkaline media. Compunds **5** and **6**, which exhibit a reasonable CL efficiency and preserve their chemiluminogenic ability in alkaline media quite well, are also interesting. The CL efficiency of nonsubstituted $MPCA^+$ (**1**) is quite high, but the compound loses its chemiluminogenic ability in alkaline media fairly quickly. Compounds **7** and **12**, i.e., $MPCA^+$ substituted with a bulky *t*-Bu group or three Me groups in the benzene ring, cannot be recommended as useful chemiluminogens since they have the lowest U values.

Chemiluminogenic Ability against Structural Features. Attempts were made to discover possible relationships between chemiluminescent characteristics, chemiluminescence quantum yields (Table 2) and usefulness (Figure 6), and factors reflecting the structural or physicochemical features of $MPCA^+$. After consideration of a number of dependencies we noted a falling trend in the plot of the chemiluminescence quantum yield versus the cavity volume (the volume of the hydration layer) of the phenyl carbonate fragment (**20** in Scheme 1) removed during the formation of electronically excited 10-methyl-9-acridinone (step VI in Scheme 1) (Figure 7). On the other hand, the values of the usefulness after 15 and 30 min of thermostatting against cavity volume

can be roughly approximated with the polynomial type dependencies shown in Figure 8. These relationships can tentatively be used to design $MPCA^+$ in the context of their utility as chemiluminogens. They indicate that optimal values of the volume of the hydration layer of the leaving group in the case of an $MPCA^+$ range between 200 and 260 $Å^3$.

Conclusions

The synthesis of 10-methyl-9-(phenoxycarbonyl)acridinium trifluoromethanesulfonates substituted with one or more alkyl groups at the benzene ring provided a unique opportunity for studying the influence of the structure of these entities on their physicochemical and chemiluminogenic features.

The basic chemiluminescent characteristics of the compounds were determined and analyzed from the point of view of their chemiluminogenic ability and susceptibility to participation in side reactions in alkaline media.

The suggested and computationally supported mechanism of chemiluminescence generation accounts for the experimental observations and reveals the pathways by which $MPCA^+$ are converted to light-emitting species and the side reactions during which they are converted to nonchemiluminescing entities. This provides a convenient framework within which to consider the chemiluminescence of acridinium cations.

Chemiluminescence quantum yields are proportional to the numbers of 10-methyl-9-(phenoxycarbonyl)acridinium cations over a wide range of concentrations (from 10^{-10} to 10^{-4} M). Detection limits are at the 10^{-10} M level. This information forms the basis for the analytical application of the compounds investigated.

Cations containing one or two Me groups in the *ortho* position of the benzene ring appeared to be the most promising chemiluminescent indicators or fragments of chemiluminescent labels. *Meta*- and *para*-substituted derivatives exhibit relatively high chemiluminescence quantum yields but are poorly resistant to alkaline media, which makes them less attractive than *ortho*-substituted derivatives. If a bulky *t*-Bu group or three Me groups are present in the benzene ring, the relevant cations are only weakly chemiluminescent.

The chemiluminescence quantum yields of $MPCA^+$ evaluated using luminol as a standard range from 0.6×10^{-2} to 2.2×10^{-2} einstein/mol; the latter value is higher than the one for luminol. Moreover, the chemiluminescence of $MPCA^+$ is initiated without a catalyst, but the latter is needed to trigger the chemiluminescence of luminol. In the case of $MPCA^+$ a better signal-to-noise ratio is also obtained. This indicates that $MPCA^+$ appear to be a suitable chemiluminogens.

Chemiluminescence quantum yields decrease with the cavity volume (the volume of the hydration layer) of the phenyl carbonate fragment, removed during the formation of light emitting 10-methyl-9-acridinone molecules. This dependency can be tentatively used for selecting $MPCA^+$ with respect to their chemiluminescence output.

The usefulness parameter, simultaneously reflecting the chemiluminogenic ability and resistance of the compounds to hydrolysis, was introduced in response to the analytical applications of $MPCA^+$. The dependencies of this quantity on the cavity volume (the volume of the hydration layer) of the phenyl carbonate fragment removed upon oxidation can be roughly fitted with polynomial relationships, which can be tentatively used for designing $MPCA^+$ in the context of their ability to chemiluminesce.

This paper combines various aspects of the chemiluminescence of 10-methyl-9-(phenoxycarbonyl)acridinium salts, which can be used as indicators of fragments of chemiluminescence labels. The finding that alkyl substituents in the phenyl fragment affect the chemiluminogenic and physicochemical features of this group of compounds has prompted the continuation of investigations into the influence of substituents with different electronic properties on these features. It is also interesting to know whether and how substituents at C(9) other than phenoxycarbonyl impart a chemiluminogenic ability to the relevant acridinium cations. These are problems that we are currently working on.

Experimental Section

Syntheses, Purification, and Analyses. Phenyl acridine-9-carboxylates (PAC) were synthesized using a modification of the method described by Sato,[10a] which enabled compounds to be obtained with a relatively high yield.[17−21] Dehydrated acridine-9-carboxylic acid (2.5 g) was converted into 9-chlorocarbonyl acridine hydrochloride by refluxing it with a 5-fold molar excess of thionyl chloride (yield 92%). Then, 0.15−0.2 g portions of the synthesized compound were stirred with a stoichiometric quantity of phenol or appropriate alkylphenol (Chart 1) in dichloromethane (5 mL) in the presence of *N*,*N*-diethylethanamine (0.4 mL) and catalytic amounts of *N*,*N*-dimethyl-4-pyridinamine (room temperature, 15−25 h, anhydrous conditions). The crude PAC (yield 60−90%) were washed with HCl, $NaHCO_3$, and NaCl solutions and purified by gravitational chromatography using a SiO_2 column (Silica Gel 60, Merck) and cyclohexane/ethyl acetate as the mobile phase (3/2 v/v). The purity of the PAC was checked by thin-layer chromatography (fluorescence detection) and their identity confirmed by elemental analysis (Table 1S, Supporting Information). Complete NMR data for all precursors of the compounds investigated are reported in ref 19, and thermoanalytic data including their melting points are listed in ref 20. The structures of the precursors of compounds **2**, **5**, and **8** were determined by the X-ray method.[21a,b]

An effective methylating agent, namely, methyl trifluoromethanesulfonate, was used to quaternarize the PAC.[31] The PAC (120 mg) were thus stirred with a 5-fold molar excess of methyl trifluoromethanesulfonate in dry dichloromethane (3.5 mL) (Ar atmosphere, room temperature, 3−4 h). Crude 10-methyl-9-(phenoxycarbonyl)acridinium trifluoromethanesulfonates were dissolved in a small amount of ethanol, filtered, and precipitated with a 25 v/v excess of diethyl ether (yield 85−92%). The purity of the compounds (**1**−**12**) was checked by HPLC (the relative areas under the main signal were >99% in all cases) and their identity confirmed by mass spectrometry (Table 1S, Supporting Information). Complete NMR data for all the compounds investigated are reported in ref 19, and their melting points are provided in ref 20. The structures of most of the salts (**1**, **2**, **4**−**7**, **9**, and **12**) were determined by X-ray methods.[21c−i,22]

Spectrophotometric Titrations. Selected compounds (**1**, **2**, and **9**) were dissolved in 10^{-3} M HCl to obtain a final concentration of $MPCA^+$ of 4×10^{-4} M. Aliquots of the latter solution (1.9 mL) were titrated at ambient temperature against sodium hydroxide solution (9.0×10^{-3} M) in steps of 0.004 mL to a final pH of 12.0, using a calibrated 0.5 mL Hamilton syringe and combined pH microelectrode calibrated prior to measurements

(31) Alder, R. W. *Chem. Ind.* **1973**, 983–986.

against at least five buffers. After the addition of gradually increasing amounts of base, the UV−vis spectra from 250 to 500 nm were recorded. By plotting absorbance at nine selected wavelengths against pH, sigmoid-type curves with one inflection point were obtained, from which the pK of the reaction $MPCA^+ + OH^- \rightarrow MPCAOH$ (corresponding to the formation of **23** (Scheme 1)) were determined using the Henderson−Hasselbach algorithm[32] implemented in the Spectral Data Lab software.[33]

Fluorometric Measurements. Chemiluminescence spectra in the 400−600 nm range at room temperature were recorded after mixing 1 mL of a 4×10^{-5} M solution of $MPCA^+$ (**1**, **2**, or **9**) in 0.001 M HCl with 0.5 mL of a 0.06% solution of H_2O_2 in 0.1 M HNO_3 in a spectrofluorimeter cuvette and adding, with continuous stirring, 0.5 mL of 0.2 M NaOH (all aqueous solutions). On completion of the reaction leading to chemiluminescence, the postreaction mixtures were left for 1 h, and fluorescence spectra were recorded at excitation wavelengths 254, 260, and 285 nm. For comparison, fluorescence spectra of 10-methyl-9-acridinone (2×10^{-5} M) were recorded under the conditions described above.

The fluorescence decay at 10-methyl-9-acridinone was recorded by a time-correlated single photon counting technique using Ludox as reference material.[34] The decay curve was fitted to the equation $I(t) = \Sigma_i \alpha_i \exp(-t/\tau_i)$, where I is the number of counts in a given time (t), α is the scaling factor (amplitude), and τ is the lifetime (the reciprocal of the unimolecular rate constant), using an iterative convolution procedure based on the least-squares method.

Chemiluminescence Investigations. To record time-dependent profiles of chemiluminescence, $MPCA^+$ was dissolved in HPLC-grade acetonitrile to a concentration of 0.005 M (stock solution). Portions of this solution were diluted with HCl (0.001 M) to obtain a concentration of 4×10^{-8} M. Aliquots (200 μL) of this solution (five samples for each compound) were placed in the 96-well white polystyrene plate of the chemiluminometer. Next, 100 μL portions of an H_2O_2 solution (0.06% w/w) in 0.1 M HNO_3 were added to each well, and the plate was shaken for 10 s. Chemiluminescence was triggered by adding 100 μL of NaOH solution (0.2 M) to each well (the final concentration of $MPCA^+$ was 2×10^{-8} M). The CL intensity−time profiles, expressed in relative light units (RLU), were measured at a photomultiplier voltage of 1000 mV over a period of time corresponding to a 99% drop in its maximum value. The influence of oxidant concentration on chemiluminescence output was investigated by adding 100 mL portions of an H_2O_2 solution (concentration 0.01−0.90%) in 0.1 M HNO_3. The CL−time profiles were also measured at 500 mV, using initial $MPCA^+$ solutions in 0.001 M HCl of concentration 4×10^{-5} M (the final concentration of $MPCA^+$ was 2×10^{-5} M).

To measure the chemiluminescence output (calibration curves), acetonitrile solutions of $MPCA^+$ (0.005 M) were diluted with 0.001 M HCl to obtain a series of solutions with concentrations from 4×10^{-8} to 4×10^{-5} M. Chemiluminescence was initiated as described above. The areas under the CL−time profiles were determined using chemiluminometer software (five samples for each compound). These areas, expressed in integral RLU, represent the relative light sums. These values are linearly dependent on the concentration of $MPCA^+$.[1c,5e] These dependencies are represented by calibration graphs, which were generated for selected compounds (**1**, **2**, and **4**).

To determine the absolute chemiluminescence efficiency, the chemiluminometer was calibrated using luminol as luminogenic standard (the spectral characteristics of luminol (range of emission 380−600 nm, λ_{max} = 435 nm) and $MPCA^+$ (range of emission 400−600 nm, λ_{max} = 455 nm) are comparable).[28] In the calibration experiments, the concentration of luminol in 0.1 M K_2CO_3 was 1.13×10^{-6} M, the concentration of H_2O_2 was 2×10^{-3} M, and the concentration of horseradish peroxidase was 2×10^{-7} M (final pH = 11.6). Knowing the chemiluminescence quantum yield (1.23×10^{-2} einstein/mol)[28] and the light sums of luminol (five replicate measurements at 99% completion of the reactions leading to light emission), the chemiluminescence quantum yields of $MPCA^+$ (ϕ_{CL}) were derived from the light sums obtained in the above manner using eq 1

$$\phi_{CL} = \frac{S_X}{S_{ST}} \times \frac{c_{ST}}{c_X} \times \phi_{ST} \quad (1)$$

where ϕ_{ST} is the chemiluminescence quantum yield of luminol, S_X is the area under the CL−time profile of $MPCA^+$, S_{ST} is the area under the CL−time profile of luminol, c_X is the concentration of $MPCA^+$, and c_{ST} is the concentration of luminol. After collection of the light sums for the standard (five replicate measurements, 99% completion of reaction, PMT voltage = 1000 mV), the light sums for $MPCA^+$ were obtained. The chemiluminescence intensities of **1**−**12**, expressed as the total number of photons emitted (N_{CL}) from a known number of molecules, were calculated using eq 2

$$N_{CL} = \frac{S_X}{S_{ST}} \times \frac{c_{ST}}{c_X} \times N_{CL,ST} \quad (2)$$

where N_{CL} is the total number of photons emitted by $MPCA^+$, S_X is the area under the CL−time profile of $MPCA^+$, S_{ST} is the area under the CL−time profile for luminol, c_X is the concentration of $MPCA^+$, c_{ST} is the concentration of luminol, and $N_{CL,ST}$ is the total number of photons emitted from 2.09×10^{14} molecules of luminol.[28]

To investigate the stability of $MPCA^+$ in basic media, the stock solutions of the compounds were diluted with buffer of pH = 8.0 to give a final concentration of 4×10^{-5} M. The solutions were thermostated at 298 K for 15 min, and 200 μL aliquots of them (five samples of each compound) were transferred to the 96-well white polystyrene plate of the chemiluminometer. Subsequently, 100 μL of 0.06% w/w H_2O_2 in 0.125 M HNO_3 was added to each well (to reach pH = 6.0), and the plate was shaken for 10 s. To trigger chemiluminescence, 100 μL of NaOH (0.3 M) was added to each well (final concentration of $MPCA^+ = 2 \times 10^{-5}$ M, final pH = 11.6). The light sums were measured as described above. The stability of $MPCA^+$, expressed as residual CL intensity, was obtained from the following equation:

$$\text{stability} = 100\% \times \text{light sum}(t = 15\ \text{min}, t = 30\ \text{min}) / \text{light sum}(t = 0\ \text{min})$$

To measure the relative CL efficiency at various pH, 50 μL aliquots of $MPCA^+$ (4×10^{-5} M, five samples of each compound) were distributed over the 96-well white polystyrene plate of the chemiluminometer. Next, a 50 μL portion of 0.12% w/w H_2O_2 in 0.01 M HNO_3 was added to each well, and the plate was shaken for 10 s. Chemiluminescence was triggered by adding 300 μL of each of the following buffers, pH = 8.0, 10.0, and 12.0, after which the

(32) (a) Albert, A.; Briggs, J. M. In *The Determination of Ionisable Constants*; Chapman and Hall: London, 1971. (b) Ossowski, T.; Goulart, M. O. F.; de Abreu, F. C.; Sant'Ana, A. E. G.; Miranda, P. R. B.; de Oliveira Costa, C.; Liwo, A.; Falkowski, P.; Zarzeczanska, D. *J. Braz. Chem. Soc.* **2008**, *19*, 175–183.

(33) Doroshenko, A. O. *Spectral Data Lab software*, Institute of Chemistry at Kharkiv National University, Kharkiv, Ukraine, 2003.

(34) O'Connor, D. V.; Philips, D. *Time-Correlated Single Photon Counting*; Academic Press: London, 1984.

(35) (a) *Atkins' Physical Chemistry*, 7th ed.; Atkins, P. W., de Paula, J., Eds.; Oxford University Press: Oxford, 2006. (b) Hadd, A. G.; Seeber, A.; Birks, J. W. *J. Org. Chem.* **2000**, *65*, 2675–2683.

light sums were measured as described above. The relative CL efficiency was calculated from the formula

$$\text{relative CL efficiency} = 100\% \times \text{light sum (pH} = 8.0, 10.0, 12.0)/\text{light sum of } \mathbf{1} \text{ (pH} = 12.0)$$

Kinetic Analysis of Time-Dependent Profiles of Chemiluminescence. The formalism of the kinetics of the two-step consecutive chemical process was adopted to describe the CL−time profiles.[35] It was assumed in this approach that chemiluminescence is generated by the process

$$\text{MPCA}^+ \xrightarrow{k_1} \text{intermediate} \xrightarrow{k_2} \text{A}^*$$

where A* stands for the electronically excited light emitting species. Using the relevant kinetic equations[35] and assuming that the intensity of emission is proportional to the concentration of A*, one obtains the expression

$$\text{CL intensity} = C\frac{k_1}{k_1 + k_2}[\exp(-k_1 t) - \exp(-k_2 t) \qquad (3)$$

in which C is a constant (expressed in RLU), t represents the time from the triggering of chemiluminescence, and t_{max} denotes the time corresponding to the maximum CL intensity:

$$t_{max} = \frac{1}{k_2 - k_1} \ln \frac{k_2}{k_1} \qquad (4)$$

The values of C, k_1, and k_2 were calculated by fitting CL−time profiles simultaneously to the two above-mentioned equations using the nonlinear least-squares method implemented in the Origin 7.5 software.[36]

MPCA$^+$ Conversion Products. To investigate the chemical changes accompanying the oxidation of MPCA$^+$ (**1**, **2** and **9**), 20 μL aliquots of stock solutions were placed in Eppendorf vials and mixed first with 50 μL of H_2O_2 solution (0.06% w/w) in 0.1 M HNO_3 and then with 50 μL 0.2 M NaOH (the final concentration of MPCA$^+$ was ca. 8.3×10^{-4} M). On completion of emission, the reactant mixtures were acidified with the addition of a drop of a 1/1 v/v trifluoroacetic acid/acetonitrile mixture and subjected to HPLC analysis (spectrophotometric detection at 268 nm). The products, 10-methyl-9-acridinone, the 9-carboxy-10-methylacridinium cation and phenol (in the case of **1**), 2-methylphenyl (in the case of **2**), or 2,6-dimethylphenol (in the case of **9**), were identified and assayed quantitatively using standard procedures. The chemical conversions of MPCA$^+$ (**1**, **2**, or **9**) in oxidant-free conditions were investigated in a similar way. Thus, 10 μL aliquots of the stock solutions were placed in Eppendorf vials and diluted with 100 μL 0.1 M HNO_3. The dark processes were initiated by the addition of 100 μL 0.2 M NaOH to the above mixtures (the final concentration of MPCA$^+$ was ca. 2.4×10^{-4} M). They were terminated at selected time intervals after initiation of the reactions (2 s to 40 min) by the addition of 20 μL of the 1/1 trifluoroacetic acid/acetonitrile mixture. The reaction mixtures obtained were subjected to HPLC analysis in order to identify the products and assay them quantitatively, as described above. The quantitative data obtained were used to analyze the kinetics of the dark processes occurring.

Quantum Chemistry Computations. Unconstrained geometry optimizations of isolated molecules were carried out at the density functional theory (DFT) level[37] using gradient techniques[38] and the 6-31G** basis set.[39] The calculations were carried out with the B3LYP functional, in which Becke's nonlocal exchange[40] and the Lee−Yang−Parr correlation functionals[41] were applied. After completion of each optimization, the Hessian (second derivatives of the energy as a function of the nuclear coordinates) was calculated to assess whether stationary structures had been obtained.[37,39b] The harmonic vibrational frequencies were then derived from the numerical values of these second derivatives and used to obtain the Gibbs' free energy contributions at 298.15 K and standard pressure with the aid of a built-in computational program of statistical thermodynamics routines.[42] The solvent effect was included in the single-point DFT calculations utilizing the polarized continuum model (PCM) (UAHF radii were used to obtain the molecular cavity).[43] With this approach, the cavity volumes (the volumes of hydration layers) of the phenyl carbonate fragments (**20** in Scheme 1) were obtained. Calculations were carried out using the Gaussian 03 program package.[44]

The enthalpies ($\Delta_{r,298}H°$) and Gibbs' free energies (free energies in the case of DFT(PCM)) ($\Delta_{r,298}G°$) of the reactions (r), as well as the enthalpies ($\Delta_{a,298}H°$) and Gibbs' free energies (free energies in the case of DFT(PCM)) ($\Delta_{a,298}G°$) of activation (a) indicated in Scheme 1 were calculated by following the basic rules of thermodynamics.[35a] The rate constants ($_{298}k°$) for the gaseous phase reactions were obtained by applying the equation

$$298^{k°} = \frac{RT}{Nh} \exp[-\Delta_{a,298}G°/(RT)] \qquad (5)$$

resulting from transition state theory, and the reaction completion time ($_{298}\tau_{99}$) from the formula

$$298^{\tau_{99}} = \ln 100/_{298}k° \qquad (6)$$

where R, T, N, and h denote the gas constant, temperature (298.15 K), Avogadro number, and Planck's constant, respectively.[4,16,35a]

Acknowledgment. This study was financed by the State Funds for Scientific Research through grant No. 4 T09A 123 23 (contract no. 0674/T09/2002/23) of the Polish State Committee for Scientific Research (for the period 2002−2005) and grant no. N204 123 32/3143 (contract no. 3143/H03/2007/32) of the Polish Ministry of Research and Higher Education (for the period 2007−2010), as well as EU Structural Funds in Poland (contract no. ZPORR/2.22/II/2.6/ARP/U/2/05 to A.O.). The purchase of the Fluoroskan Ascent FL fluoroluminometer was possible as a result of financial support from the Foundation for Polish Science − IMMUNO'99 program (contract no. 61/99). We thank Dr M. Gołębiewski for recording the MS spectra. DFT calculations were carried out on the computers of the Tri-City Academic Network Computer Centre (TASK) in Gdansk (Poland).

(36) *Origin 7.5*, Origin Lab Co., Northampton, MA, 1991−2004.
(37) *Density Functional Methods in Chemistry*; Labanowski, J. K., Andzelm, J. W., Eds; Springer-Verlag: New York, 1991.
(38) *Modern Electronic Structure Theory: Geometry Optimization on Potential Energy Surfaces*; Schlegel, H. B., Ed.; World Scientific Publishing: Singapore, 1994.
(39) (a) Hariharan, P. C.; Pople, J. A. *Theor. Chim. Acta* **1973**, *28*, 213–222. (b) Hehre, W. J.; Radom, L.; Schleyer, P. v. R.; Pople, J. A. *Ab Initio Molecular Orbital Theory*; Wiley: New York, 1986.
(40) (a) Becke, A. D. *Phys. Rev. A* **1988**, *38*, 3098–3100. (b) Becke, A. D. *J. Chem. Phys.* **1993**, *98*, 1372−1377, 5648–5652.
(41) Lee, C; Yang, W; Parr, R. G. *Phys. Rev. B* **1988**, *37*, 785–789.
(42) Dewar, M. J. S.; Ford, G. P. *J. Am. Chem. Soc.* **1977**, *99*, 7822–7829.
(43) (a) Tomasi, J.; Persico, M. *Chem. Rev.* **1994**, *94*, 2027–2094. (b) Barone, V.; Cossi, M.; Mennucci, B; Tomasi, J. *J. Chem. Phys.* **1997**, *107*, 3210–3221.
(44) Frisch, M. J. et al. *Gaussian 03*, revision C.02; Gaussian, Inc.: Wallingford, CT, 2004.

Supporting Information Available: Elemental analyses of **1**−**12**; MS data (molecular ions); retention factors (TLC); retention times (HPLC); composition of post-CL reaction mixtures (HPLC); retention time vs partition coefficient relationships; FAB mass spectrum of **1**; stationary fluorescence spectra of light-emitting mixtures (**1**, **2**, and **9**); stationary fluorescence spectra of post-CL mixtures (**1**, **2**, and **9**) together with the spectrum of 10-methyl-9-acridinone; fluorescence decay spectrum of 10-methyl-9-acridinone; chemiluminescence intensity profiles (**1**) at various H_2O_2 concentrations; relationships between CQY (**1**, **2**, and **4**) and H_2O_2 concentration; DFT-optimized geometries of entities involved in the reaction mechanism of $MPCA^+$ (**1**, **2**, and **9**) with OOH^- and OH^- or appearing in the text; chromatograms of post-CL reaction mixtures (**2**); UV−vis spectra of spectrophotometric titrations (**1**); Cartesian coordinates and values of thermodynamic characteristics of all the molecules investigated. This material is available free of charge via the Internet at http://pubs.acs.org.